

SUPPLEMENTAL MATERIAL

Methods

Immunofluorescence staining. Human right atrial appendage tissue was placed in Tyrode's solution. Tissue was then cryopreserved and sectioned at 10µm thickness. For all immunofluorescence staining, the slides were air dried for 5 minutes, fixed in formalin for 30 minutes, and washed in PBS, 3 times, 5 minutes each. The sections were incubated with a blocking buffer (3% gelatin from cold water fish skin, 0.1% Triton X, and 2 mg/ml BSA in PBS) with normal serum. The tissue was incubated overnight in the primary antibody (rabbit anti-mouse ox-CaMKII). The next day slides were washed in PBS and the tissue incubated with appropriate secondary antibodies for 1 hour. The slides were then washed and cover-slipped with VECTASHIELD (Vector Laboratories) with DAPI mounting medium.

Immunoblotting for human samples. Patient atrial myocardium was homogenized in Tris buffer as previously reported⁹ containing (in mM) Tris-HCl 20, NaCl 200, NaF 20, Na₃VO₄ 1, DTT 1, 1% Triton X-100 (pH 7.4) and complete protease-inhibitor cocktail (Roche). Protein concentration was determined by BCA assay (Pierce Biotechnology). Protein concentration was adjusted to 1 µg/µl with phosphate buffered saline (PBS) and 5 X Laemmli buffer without β-mercaptoethanol was added (1:20) and samples were heated to 95°C for 30 min. Denaturated tissue homogenates were subjected to Western blotting (8% SDS-polyacrylamide gels) using anti-CaMKII (1:15000, gift from D. M. Bers, University of California, Davis, CA) and anti-ox-CaMKII (1:15000) antibodies.

Chemi-luminescent detection was done with SuperSignal West Pico Substrate (Pierce).

Mouse Models and Experimental Methods. $p47^{-/-}$ mice were purchased from Jackson Labs. Mice with transgenic myocardial CaMKII inhibition (AC3-I)¹, MM-VV knock-in mice² and MsrA transgenic mice³ were generated by our laboratory as described. S2814A knock-in mice were generated by the Wehrens laboratory.⁴ All animal studies were reviewed and approved by the IACUC of the University of Iowa.

HR and BP measurements. One week prior to the start of each experiment, mice were trained on the tail cuff BP equipment (Visitech BP-2000 blood pressure analysis system). HR and BP recorded for four consecutive days. The readings from days 1-2 were discarded and days 3-4 were averaged for the baseline value. Saline or Ang II pumps were implanted after collecting the baseline data. HR and BP were measured for at least 4 days a week (to maintain habituation to the apparatus and handling) for 3 weeks. The last 3 days of data were averaged to assess the effect of 3 weeks of treatment.

Mini-osmotic pump implantation. Mini-osmotic pumps (Alzet model 1004, 0.11 μ l/hr, 28 days) containing saline or Ang II (2000 ng/kg/min) were inserted subcutaneously under anesthesia (ketamine/xylazine- 87.5/12.5 mg/kg), as previously reported.⁵

Transthoracic Echocardiography: We recorded transthoracic echocardiograms in conscious mice three weeks after Ang II pump implantation, as previously

described.⁶ Images were acquired and analyzed by an operator blinded to mouse genotype and treatment.

In vivo Electrophysiology (EP studies). Mice were anesthetized with isoflurane (2% for induction and 1.5% for maintenance of anesthesia; Isotec100 Series Isoflurane Vaporizer; Harvard Apparatus). During EP studies the mouse body temperature was monitored by an intra-rectal probe and controlled using mousepad circuit board equipped with a heating element (Mousepad, THM 100, Indus Instruments, USA). All studies were performed at $37.0 \pm 0.5^{\circ}\text{C}$. We used a Millar 1.1F octapolar EP catheter (EPR-800; Millar Instruments) inserted via the right jugular vein, as previously described.^{4,7} A computer-based data acquisition system (Powerlab 16/30; ADI instruments) was used to record a 1-lead body surface ECG and up to 4 intracardiac bipolar electrograms (Labchart Pro software, version 7; AD Instruments). In brief, right atrial pacing was performed using 2 ms current pulses delivered by an external stimulator (STG-3008; Multi Channel Systems). Using an automated stimulator, inducibility of atrial fibrillation was tested by decremental burst pacing. Burst pacing started at a 40 ms cycle length, decreasing by 2 ms every 2 seconds to a cycle length of 20 ms. Burst pacing was repeated one minute after the previous burst concluded or the termination of AF. Burst pacing was performed for a total of five times in each mouse. AF was defined as the occurrence of rapid and fragmented atrial electrograms with irregular AV-nodal conduction and ventricular rhythm for at least 1 second. If at least 2 bursts (out of 5) produced AF, the mouse was considered inducible. Mice with < 2 bursts of AF were considered non-inducible.

Immunoblotting for mouse samples. Mice were sacrificed at the end of Ang II or saline infusion 3 weeks after implantations of the mini-osmotic pumps. Hearts were excised, and the atria were separated from the ventricles and flash frozen in liquid nitrogen. Atria were then homogenized in modified RIPA buffer (50 mM HEPES, pH 7.4, 150 mM NaCl, 5 mM EDTA, 1% v/v NP-40, and 0.5% w/v deoxycholate), containing a mixture of protease and phosphatase inhibitors. Equal amounts of protein were fractionated on NuPAGE Bis-Tris gels (Invitrogen) and transferred onto PVDF membranes (Bio-Rad). After blocking nonspecific binding with 5% w/v non-fat milk powder in TBS-T (50 mM Tris-HCl, pH 7.6, 150 mM NaCl, and 0.1% v/v Tween-20), blots were incubated in primary antibodies (ox-CaMKII [1:500] and CaMKII [1:250]) overnight at 4°C. The same procedure was applied for atrial immunoblots from untreated MsrA transgenic and WT littermate mice incubating with a primary anti-MsrA antibody (1:1000, abcam). Blots were washed in TBS-T and incubated with appropriate HRP-conjugated secondary antibodies. Protein bands were detected using ECL reagent (Lumi-Light, Roche), and loading was monitored by Coomassie staining of the blots after antibody probing. Atrial lysates from Ang II treated mice were run side by side on the same gel with lysates from saline treated mice from the same genotype. Quantification was performed using Image J analysis software (version 1.46, NIH).

ROS detection. Murine left atria, acquired as described above, were mounted and flash frozen in Tissue Freezing Medium (Triangle Biomedical Sciences, Durham). The tissue was then cryo sectioned (30 µm), rinsed with PBS and

incubated in DHE (2×10^{-2} M, Invitrogen) for 15 minutes at room temperature in darkness as previously described with minor alterations.⁸ Fluorescence was measured using a laser scanning confocal microscope (Zeiss 510 and 710; excitation at 488 nm and detection at 585 nm by using a long-pass filter). For quantification and analysis, tissue fluorescence was corrected for the nuclear fluorescence signal and normalized to the area of the imaged tissue section using Image J analysis software (version 1.46, NIH).

Atrial myocyte isolation. Atrial myocytes were isolated from adult mouse hearts using an established protocol with minor modifications.⁹

Voltage clamp. Voltage and current signals were measured with an Axon 200B patch-clamp amplifier controlled by a personal computer using a Digidata 1320A acquisition board driven by pClamp 8.0 (Axon Instruments). We used perforated (amphotericin B) patch for I_{Ca} and action potential studies.¹⁰ All experiments were conducted at $T=35^{\circ}\text{C}$. Recording pipettes, fabricated from borosilicate glass, had tip diameters of 2–3 μm and resistance of 2–4 $\text{M}\Omega$, when filled with recording solution. All solutions were adjusted to 275–295 mOsm.

Ca²⁺ Imaging. Calcium imaging was performed as described previously.¹¹ Briefly, atrial myocytes were loaded with Fluo-3 AM (5 μM , 20 min) at room temperature. After de-esterification, the cells will be perfused with normal Tyrode solution (1.8 mM Ca^{2+}). Confocal Ca^{2+} imaging will be performed with a laser scanning confocal microscope (LSM 510 Meta, Carl Zeiss) equipped with a NA=1.35, 63x lens. Line-scan measurement of Ca^{2+} transients, SR content and sparks were acquired at a sampling rate of 1.93 ms/line along the longitudinal

axis of the myocytes. Ca^{2+} sparks were measured under resting conditions. Steady state Ca^{2+} transients were achieved by a 30 sec pacing at 1 Hz. Sarcoplasmic reticulum Ca^{2+} content was measured as a global Ca^{2+} release induced by 20 mM caffeine. All digital images were processed with IDL 6.0 (Research System Inc).

Statistics. Data are presented as mean \pm SEM. P values were assessed with a Student's t-test (2-tailed), ANOVA or two-way ANOVA, as appropriate, for continuous data. Post hoc comparisons after ANOVA were performed using the Bonferroni test. Discrete variables were analyzed by Fisher's exact test. The null hypothesis was rejected for $p < 0.05$. From the fitted ANOVA model, tests of mean contrast were performed to test for differences between Ang II versus saline within each genotype (mouse strain) with p-values adjusted using Bonferroni's method to account for the number of tests performed (i. e. adjusted for 4 tests corresponding to each genotype). Similarly, tests of mean contrast were also used for pair-wise comparison of the Ang II versus saline differences between the genotypes with the p-value adjusted using the Bonferroni step-down method (adjusted for pairwise comparisons among all genotypes, or a total of 6 comparisons). The two-way ANOVA was performed on the natural log (Ln) transformation of the (normalized to Coomassie) ox-CaMKII, CaMKII, and ox-CaMKII/CaMKII ratio data. This was done because the data were not normally distributed and there was inequality of variance among the genotype-treatment groups. By applying the Ln transformation, the data distribution was normalized and homogeneity of variance was achieved. Since the mean estimates from the

ANOVA are in the Ln transformed scale, these were back-transformed to obtain means in the original scale, which corresponds to the geometric mean. The ratio of Ang II relative to saline group means in the original scale were computed by back-transformation of the difference between Ang II and saline treatment group means in the Ln scale.

References

1. Zhang R, Khoo MSC, Wu Y, Yang Y, Grueter CE, Ni G, Price EE, Thiel W, Guatimosim S, Song L-S, Madu EC, Shah AN, Vishnivetskaya TA, Atkinson JB, Gurevich VV, Salama G, Lederer WJ, Colbran RJ, Anderson ME. Calmodulin kinase II inhibition protects against structural heart disease. *Nat Med.* 2005;11:409–417
2. Luo M, Guan X, Luczak ED, Lang D, Kutschke W, Gao Z, Yang J, Glynn P, Sossalla S, Swaminathan PD, Weiss RM, Yang B, Rokita AG, Maier LS, Efimov IR, Hund TJ, Anderson ME. Diabetes increases mortality after myocardial infarction by oxidizing CaMKII. *J Clin Invest.* 2013;123:1262–1274
3. He BJ, Joiner M-LA, Singh MV, Luczak ED, Swaminathan PD, Koval OM, Kutschke W, Allamargot C, Yang J, Guan X, Zimmerman K, Grumbach IM, Weiss RM, Spitz DR, Sigmund CD, Blankesteyn WM, Heymans S, Mohler PJ, Anderson ME. Oxidation of CaMKII determines the cardiotoxic effects of aldosterone. *Nat Med.* 2011;17:1610–1618
4. Chelu MG, Sarma S, Sood S, Wang S, van Oort RJ, Skapura DG, Li N, Santonastasi M, Müller FU, Schmitz W, Schotten U, Anderson ME, Valderrábano M, Dobrev D, Wehrens XHT. Calmodulin kinase II-mediated sarcoplasmic reticulum Ca^{2+} leak promotes atrial fibrillation in mice. *J Clin Invest.* 2009;119:1940–1951

5. Erickson JR, Joiner M-LA, Guan X, Kutschke W, Yang J, Oddis CV, Bartlett RK, Lowe JS, O'Donnell SE, Aykin-Burns N, Zimmerman MC, Zimmerman K, Ham A-JL, Weiss RM, Spitz DR, Shea MA, Colbran RJ, Mohler PJ, Anderson ME. A dynamic pathway for calcium-independent activation of CaMKII by methionine oxidation. *Cell*. 2008;133:462–474
6. Weiss RM, Ohashi M, Miller JD, Young SG, Heistad DD. Calcific aortic valve stenosis in old hypercholesterolemic mice. *Circulation*. 2006;114:2065–2069
7. Verheule S, Sato T, Everett T, Engle SK, Otten D, Rubart-von der Lohe M, Nakajima HO, Nakajima H, Field LJ, Olgin JE. Increased vulnerability to atrial fibrillation in transgenic mice with selective atrial fibrosis caused by overexpression of TGF-beta1. *Circ Res*. 2004;94:1458–1465
8. Swaminathan PD, Purohit A, Soni S, Voigt N, Singh MV, Glukhov AV, Gao Z, He BJ, Luczak ED, Joiner M-LA, Kutschke W, Yang J, Donahue JK, Weiss RM, Grumbach IM, Ogawa M, Chen P-S, Efimov I, Dobrev D, Mohler PJ, Hund TJ, Anderson ME. Oxidized CaMKII causes cardiac sinus node dysfunction in mice. *J Clin Invest*. 2011;121:3277–3288
9. Koval OM, Guan X, Wu Y, Joiner ML, Gao Z, Chen B, Grumbach IM, Luczak ED, Colbran RJ, Song LS, Hund TJ, Mohler PJ, Anderson ME. CaV1.2 -subunit coordinates CaMKII-triggered cardiomyocyte death and afterdepolarizations. *Proc Natl Acad Sci USA*. 2010;107:4996–5000

10. Wu Y, Gao Z, Chen B, Koval OM, Singh MV, Guan X, Hund TJ, Kutschke W, Sarma S, Grumbach IM, Wehrens XHT, Mohler PJ, Song L-S, Anderson ME. Calmodulin kinase II is required for fight or flight sinoatrial node physiology. *Proc Natl Acad Sci USA*. 2009;106:5972–5977
11. Guatimosim S, Guatimosim C, Song L-S. Imaging Calcium Sparks in Cardiac Myocytes. In: *Methods in molecular biology* (Clifton, N.J.). Totowa, NJ: Humana Press; 2010. p. 205–214.

Figure legend for supplementary figures:

Supplementary Figure 1. Subgroup analysis of CaMKII expression in

patients. Immunoblotting was performed on atrial tissue obtained from patients in SR and AF using antisera against ox-CaMKII **(A)** and total CaMKII **(B)**.

Patients with AF were divided into two subgroups based on their use of angiotensin converting enzyme inhibitors (ACE-i) or angiotensin receptor blockers (ARB), and the respective ox-CaMKII **(A)** and total CaMKII **(B)** levels were compared with levels in the SR group (*p<0.05 and p values as shown above, one-way ANOVA with post-hoc Tukey test). The % values indicate the mean ox-CaMKII/GAPDH ratio (panel A) and CaMKII/GAPDH ratio (panel B) in the subgroups as normalized to the corresponding mean values in the SR groups. **C.** Complete films for total CaMKII and GAPDH immunoblots with red boxes highlighting the bands shown in Figure 1E. All lanes were included in the analysis. **D.** Complete films for ox-CaMKII and GAPDH immunoblots with red boxes highlighting the bands shown in Figure 1C.

Supplementary Figure 2. Characterization of MM-VV mice.

A. Similar increase in Ca^{2+} and calmodulin independent CaMKII activity with Isoproterenol treatment (daily injections) in WT and MM-VV mice, but no increase with Ang II in MM-VV mice as compared to WT littermates (*p<0.05 ANOVA, post-hoc Tukey test). **B.** MM-VV and WT mice had similar body weights at 8 weeks of age. **C.** Similar baseline heart rates (HR) in Langendorff-perfused hearts from WT and MM-VV mice at 8 weeks of age. **D.** Similar increases in HR

(% over baseline shown in E) in response to 10 mM isoproterenol (Student's t-test) between WT and MM-VV Langendorff-perfused hearts.

Supplementary Figure 3. Atrial CaMKII and MsrA expression

A. Immunoblots for total CaMKII from atrial lysates isolated from mice treated with Ang II or saline for 3 weeks. For quantification, CaMKII bands were normalized to the total protein loading as assessed with Coomassie staining of the membrane. **B.** Summary data for total CaMKII expression in Ang II treated mice relative to saline treated mice of the same genotype. From each genotype 4 saline treated mice were used as controls. ** $p < 0.01$ versus WT saline, in addition $p = 0.002$ for WT Ang II versus MsrA TG Ang II and $p = 0.013$ for WT Ang II versus $p47^{-/-}$ Ang II. Data were analyzed using two-way ANOVA (for treatment and genotype) with Bonferroni post-hoc comparison. **C.** Immunoblots for MsrA from atrial lysates isolated from MsrA TG and WT littermates. Coomassie staining of the membrane was used as a loading control.

Supplementary Figure 4. Atrial ROS in Ang II and saline treated mice.

A. Representative DHE fluorescence images taken in cryo-preserved left atrial myocardium from WT, MM-VV, $p47^{-/-}$ and MsrA TG mice after 3 weeks of Ang II or saline infusion. Horizontal calibration bars indicate 100 μ m. **B.** Summary of left atrial DHE fluorescence data. For each genotype, the bars represent the mean intensity of DHE fluorescence in the Ang II group as relative to DHE fluorescence in the saline group. From each genotype 4 saline treated mice were

used as controls. * $p < 0.05$ versus saline from the WT and the MM-VV group separately.

Supplementary Figure 5. L-type Ca^{2+} current facilitation. **A.** Peak L-Type Ca^{2+} currents recorded from atrial myocytes of WT and MM-V mice (N=2 and 3 mice per group, respectively). **B.** Summary data for maximal facilitation of L-Type Ca^{2+} currents. Atrial myocytes from WT and MM-VV mice show similar peak L-type Ca^{2+} current density and facilitation (same amount of mice per group as in A). Facilitation is abolished by the CaMKII inhibitor KN-93 (500nM). * $p < 0.001$ for WT versus WT + KN-93 and for MM-VV versus MM-VV + KN-93, and # $p < 0.05$ WT versus MM-VV (Student's t-test). Each point represents an N=5-7 cells. **C.** Exemplary L-Type Ca^{2+} current tracings from the 1st and 4th voltage command step (-40 to 0 mV) in panel B to demonstrate facilitation.

Supplementary Figure 6. Hypertrophic response to Ang II.

LV mass as estimated by echocardiography performed after 3 weeks of Ang II or saline treatment (all comparisons versus saline controls, * $p < 0.05$ and *** $p < 0.001$, Student's t-test).

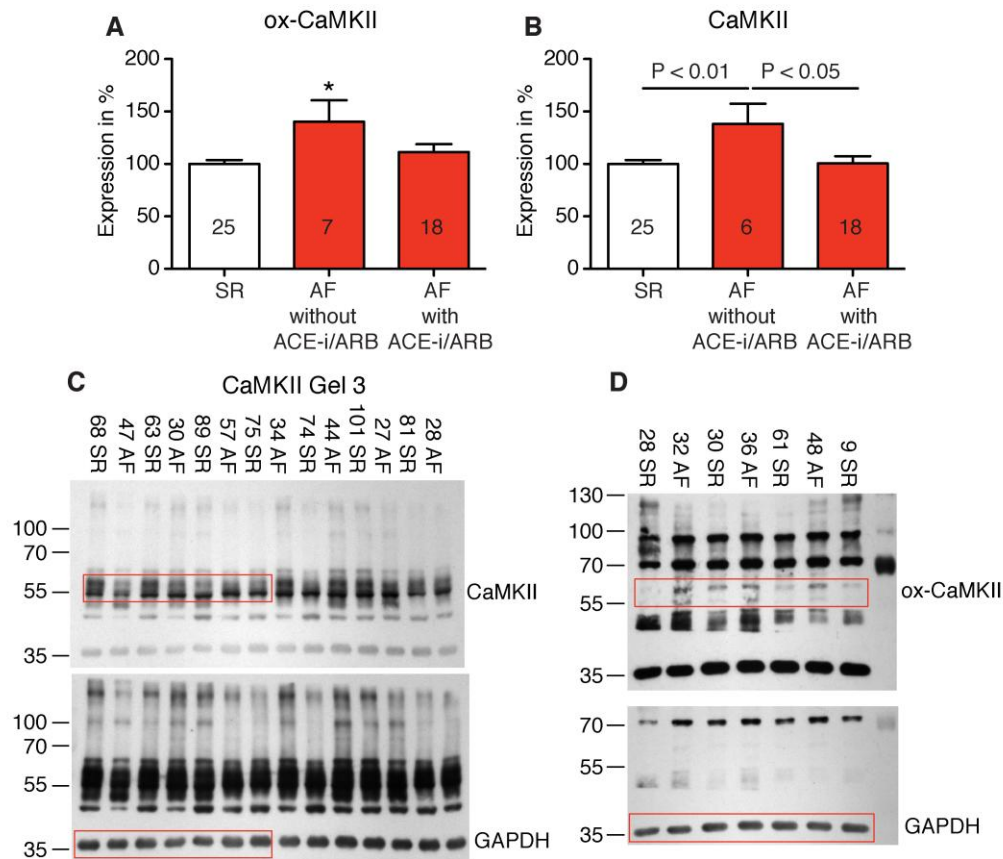
Supplementary Figure 7. Ca^{2+} spark parameters and sarcoplasmic reticulum Ca^{2+} content in WT mice.

A. Average spatial width (FWHM, full-width at half-maximal amplitude in μm). **B.** Average duration (FDHM, full duration at half-maximal amplitude in ms). **C.** Average amplitude of spontaneous Ca^{2+} sparks in WT atrial myocytes treated with 3 weeks of Ang II or saline. Ang II N=46 cells from 6 mice and saline N=23

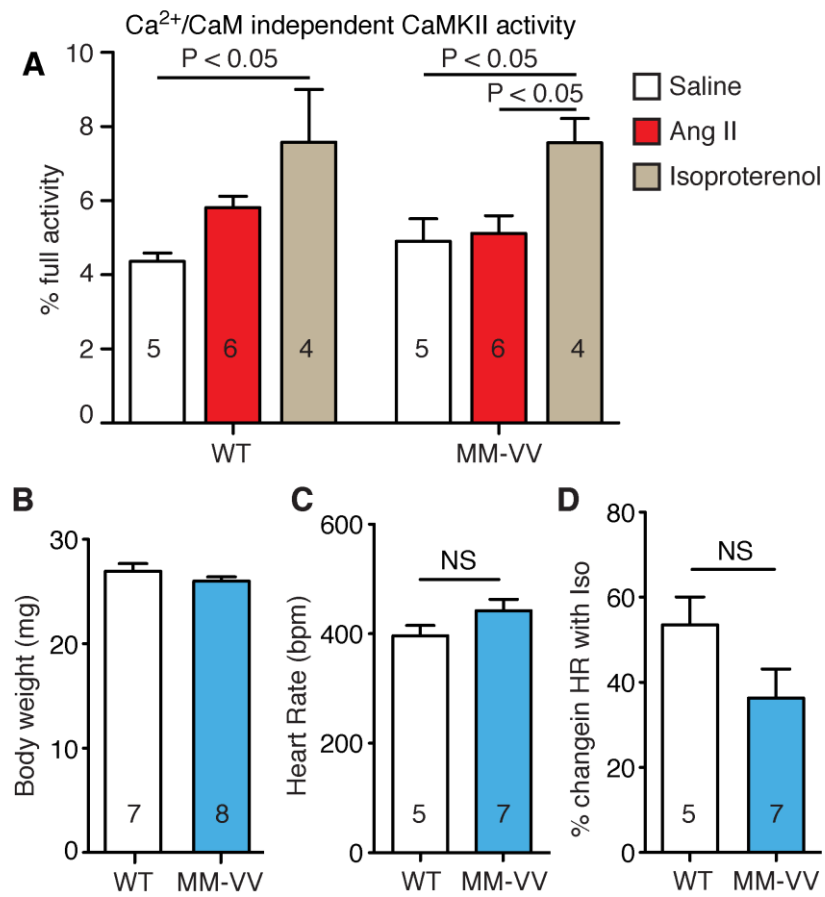
cells from 5 mice; no significant differences between Ang II and saline treatments. **D.** Sarcoplasmic reticulum (SR) Ca^{2+} transient and Ca^{2+} content (rapid SR depletion with 20 mM caffeine spritz) were similar in atrial myocytes from Ang II and WT saline treated mice (N=4 mice each group).

Supplementary Figures

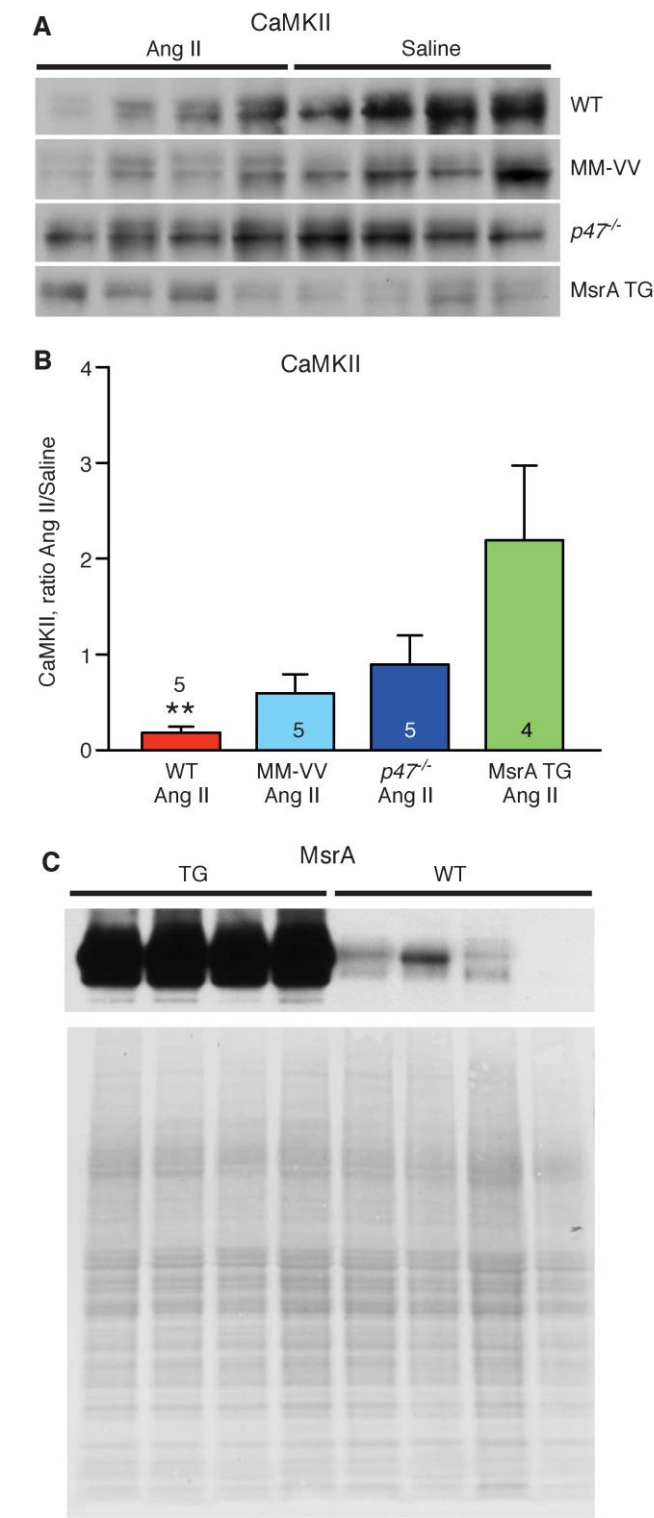
Supplementary Figure 1



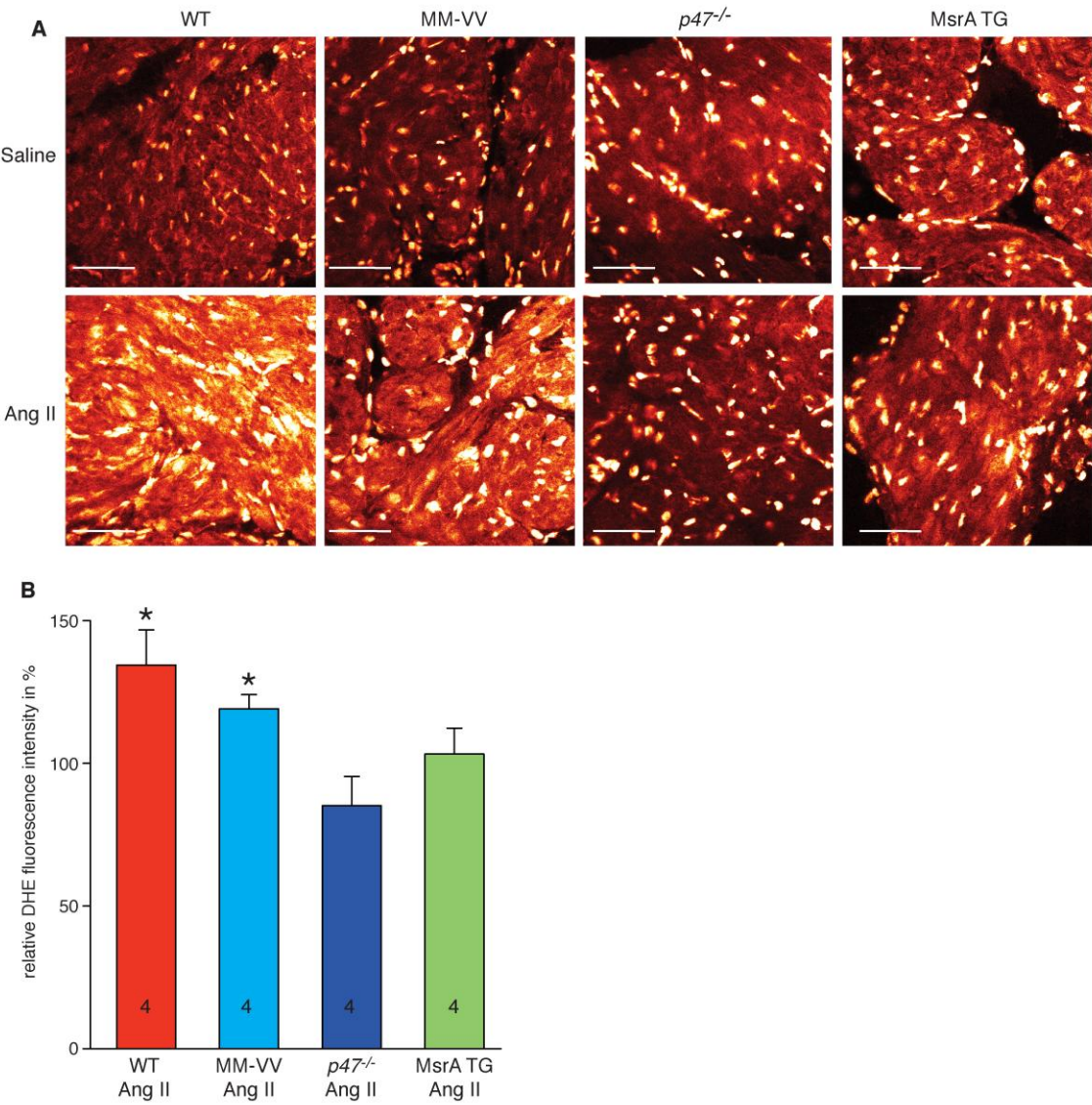
Supplementary Figure 2



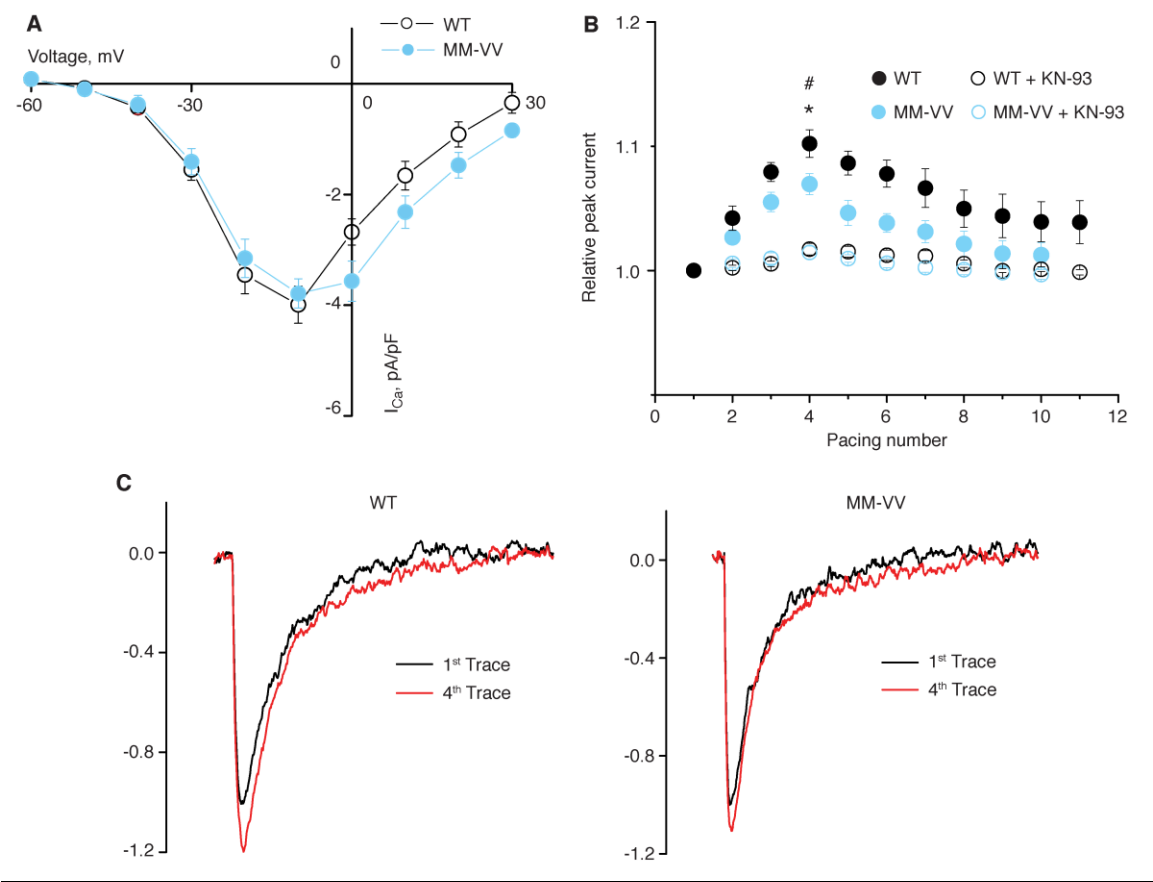
Supplementary Figure 3



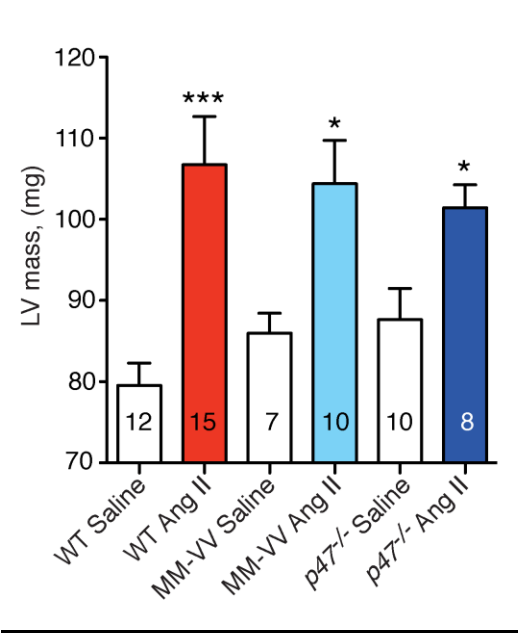
Supplementary Figure 4



Supplementary Figure 5



Supplementary Figure 6



Supplementary Figure 7

